International Journal of Engineering, Mathematical and Physical Sciences
ISSN: 2517-9934
Vol:9, No:7, 2015

Multiple-Channel Piezoelectric Actuated Tunable Optical Filter for WDM Application

Hailu Dessalegn, T. Srinivas

***Abstract*—**We propose new multiple-channel piezoelectric (PZT) actuated tunable optical filter based on racetrack multi-ring resonators for wavelength de-multiplexing network applications. We design tunable eight-channel wavelength de-multiplexer consisting of eight cascaded PZT actuated tunable multi-ring resonator filter with a channel spacing of 1.6nm. The filter for each channel is basically structured on a suspended beam, sandwiched with piezoelectric material and built in integrated ring resonators which are placed on the middle of the beam to gain uniform stress and linearly varying longitudinal strain. A reference single mode serially coupled multi stage racetrack ring resonator with the same radii and coupling length is designed with a line width of 0.8974nm with a flat top pass band at 1dB of 0.5205nm and free spectral range of about 14.9nm. In each channel, a small change in the perimeter of the rings is introduced to establish the shift in resonance wavelength as per the defined channel spacing. As a result, when a DC voltage is applied, the beams will elongate, which involves mechanical deformation of the ring resonators that induces a stress and a strain, which brings a change in refractive index and perimeter of the rings leading to change in the output spectrum shift providing the tunability of central wavelength in each channel. Simultaneous wave length shift as high as 45.54pm/**V** has been achieved with negligible tunability variation in the eight channel tunable optical filter proportional to the DC voltage applied in the structure, and it is capable of tuning up to 3.45nm in each channel with a maximum loss difference of 0.22dB in the tuning range and out of band rejection ratio of 35dB, with a low channel crosstalk ≤ 30 dB.

***Keywords*—**Optical MEMS, piezoelectric (PZT) actuation, tunable optical filter, wavelength de-multiplexer.

I. Introduction

TUNABLE optical filters are key components in wavelength-division-multiplexing networks. Such components are important to increase the bit rate for high capacity optical networks and also in switching functions for efficient signal routing. [1]. it adopts a mean to bring about change in the wavelength selection, such as index alteration and light path variation. [2].

Recent active research in the microring resonators rose interests in the tunable optical filters, especially in the photonic integrated circuits [3], [4], where the high quality factor of the microring resonator is beneficial for the good filter characteristics [5]. So far, tunable wavelength filters have been reported in a number of materials utilized the index change for the wavelength tuning, such as the termoptic effect, electroptic effect, and MEMS based tuning schemes, [6]-[9].

The wavelength tuning based on the termoptic effect, however, requires local heating and demands high standing power consumption. The electroptic effect is found only in a limited number of materials. Whereas, MEMS based tuning consumes negligible standing power if a certain actuation mechanism is used, such as electrostatic and piezoelectric, those mechanisms do not require any current flow in maintaining the actuated states. In addition, it can be implemented for a much broader range of materials than those tuning methods mentioned earlier. Finally, its tuning speed can be much faster than that of the termoptic devices.

In this paper we focused on the design, simulation and analysis of a novel, multiple-channel PZT actuated tunable optical filter based on racetrack multi-ring resonators for wavelength de-multiplexing applications. Which generate a simultaneous wavelength shift of a wave propagating in the micro resonator arrays proportional to the DC voltage applied in the structure. The device model was simulated using a commercial finite element analysis tool Comsol Multiphysics and Matlab. Theoretical and simulation results are presented. The optimum design relationships are obtained.

II. Eight-Channel PZT Actuated Tunable Filter

The architecture of the proposed wavelength de-multiplexer is designed in a cascaded piezoelectric (PZT) actuated tunable filters as shown in Fig. 1. The design of each filter involves the design of piezoelectric actuated beam, optical integrated ring resonator and opto-mechanical coupling between them. It is basically structured on a sandwiched beam, piezoelectric material (PZT-5A) sandwiched between two SiO_2 layers and built in optical integrated ring resonator which is placed on the middle of each beam to gain uniform stress, linearly varying displacement on the longitudinal direction and ideally, zero displacement on the other directions.

When a DC voltage is applied longitudinally, the beams will elongate, which involves mechanical deformation in the ring resonator arrays that induces a stress and strain, which brings a change in refractive index and perimeter of the rings leading to change in the output spectrum shift providing the tenability of central wavelength in each channel.

Hailu Dessalegn is with the Indian Institute of Science, Bangalore-560012, India (phone: (+91) 886-152-7511; fax: (+91) 802-360-0563; e-mail: hailudessalegn@yahoo.com or hailud@ece.iisc.ernet.in).

T. Srinivas is with the Indian Institute of Science, Bangalore-560012, India (phone: 974-092-2377; fax: (+91) 802-360-0563; e-mail: tsrinu@ece.iisc.ernet.in).

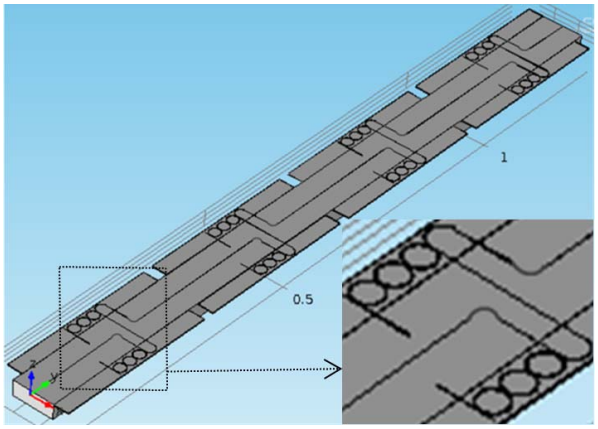

Fig. 1 Schematic of eight-channel PZT actuated wavelength de-multiplexer

A. Serially Coupled Racetrack Multi-Ring Resonator

A single mode silicon waveguide with a thickness to be 0.450μm and depth 0.220μm were designed for low loss of about 2dB/cm. A reference's serially coupled three stage racetrack ring resonators is configured, with the same radii of 10μm and directional coupler length of 4.1737μm (L_{c0}). Within each section of the three rings, the ring were nominally identical, with apodized waveguide resonator coupling coefficients, formed by varying the inter-waveguide gap in the directional couplers, from 200nm(s_0) for first and last couplers to 335nm(s_1) in the middle. Thus, the coupling efficiency is defined:

$$K_0 = K_3 = \sin(K_{abso}.L_{c0})^2 \quad (1)$$

$$K_1 = K_2 = \sin(K_{abs1}.L_{c0})^2 \quad (2)$$

where, K_{abso} is the coupling coefficient of directional coupler as s_0 the inter waveguide gap, and K_{abs1} is the coupling coefficient of directional coupler as s_1 the inter waveguide gap, and L_{c0} is the coupling length without any loud.

The proper choice of β value for the ring resonator has been worked out by using effective index method and Modified Newton approximation technique. Hence, n_{eff}= *2.2825* at 1550nm is taken for the desired single mode waveguide structure and also, we investigated and found the coupling efficiency to be $K_0 = K_3 = 34.55\%$ and $K_1 = K_2 = 2.22\%$ with negligible loss to gain a flat top pass band filter as shown in Fig. 2. For simplification, the calculation of the intensity relation does not take into account coupling losses ($\gamma = 0$). The intensity transfer function for a three-ring resonator is.

$$T = t_0.t_1.t_2.t_3.e^{(\delta_{01}+\delta_{12}+\delta_{33})} \quad (3)$$

$$D = 1 - r_0.r_1.e^{(\delta_{01}+\delta_{10})} - r_1.r_2.e^{(\delta_{12}+\delta_{21})} - r_2.r_3.e^{(\delta_{23}+\delta_{32})} - r_0.r_1.(t_1^2 - r_1^2).e^{(\delta_{01}+\delta_{10}+\delta_{12}+\delta_{21})} - r_1.r_3.(t_2^2 - r_2^2).e^{(\delta_{12}+\delta_{21}+\delta_{23}+\delta_{32})} - r_0.r_3.(t_1^2 - r_1^2).(t_2^2 - r_2^2).e^{(\delta_{01}+\delta_{10}+\delta_{12}+\delta_{21}+\delta_{23}+\delta_{32})} + r_0.r_1.r_2.r_3.e^{(\delta_{01}+\delta_{10}+\delta_{23}+\delta_{32})} \quad (4)$$

$$\delta_{jk} = -\left(\frac{\alpha}{2} + i\beta\right).L_{jk}, \text{ for } j,k = 0,1,2,3 \text{ and } i = \sqrt{-1}$$

$$I_{out} = \frac{|T|^2}{|D|^2} \quad (5)$$

where, $t_j = \sqrt{(1-K_j)(1-\gamma)}$ effective transmition coefficient of the coupler, $r_j = \sqrt{K_j(1-\gamma)}$ effective reflection coefficient of the coupler, K_i is the coupling coefficient for j=0, 1, 2 and 3 respectively, and β and α is the propagation constant and attenuation constant of a waveguide respectively.

B. Eight-Channel Dropping Filter

Here, it employed a simplest method to achieve multiple-channel filters consisting of serially coupled racetrack ring resonator arrays in silicon, where the individual resonance wavelength of each racetrack multi-ring resonator in the array is shifted by changing its perimeter [4].

Race-track shaped multi-ring resonators were chosen for analysis, and design. The reference resonator's perimeter is $P=2\times(L_{c0}+\pi R)$. The perimeter is varied by adjusting the radii of the curved portions of the racetrack multi-ring resonator from R to R+ΔR, i.e., $\Delta P=2\pi\times\Delta R$, while the coupling lengths (L_{c0}) are kept constant.

As the silicon waveguide has very large dispersion, the effective index varies when the resonance wavelength changes. Then, the resonance condition for the two resonators shown with a dotted line in Fig. 1 is

$$m\lambda_o = 2\pi R n_b + 2L_{c0}n_s \quad (6)$$

$$m(\lambda_o + \Delta\lambda) = 2\pi(R + \Delta R)(n_b + \Delta n_b) + 2L_{c0}(n_s + \Delta n_s)) \quad (7)$$

where m is an integer (resonance order), λ_o is the reference resonating wavelength, n_s is the effective index in the straight waveguide, and n_b is the effective index in the bending waveguide.

As it is outlined in paper [4], the resonance frequency shift Δλ can be approximated as:

$$\Delta\lambda_i = \left(\lambda_i \frac{\Delta P}{P}\right) / \left(1 - \frac{\lambda_o}{n_e} \times \frac{n_{e(i+1)} - n_{e(i)}}{\lambda_{(i+1)} - \lambda_{(i)}}\right) \quad (8)$$

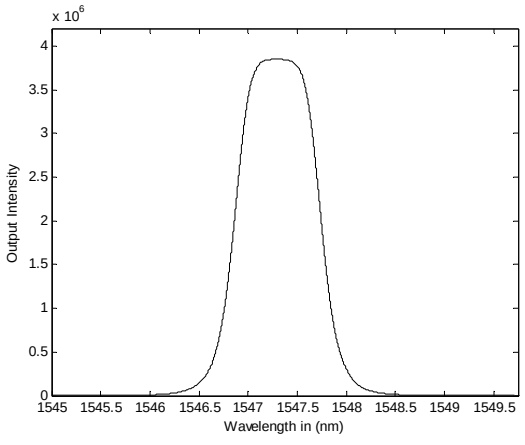

(a)

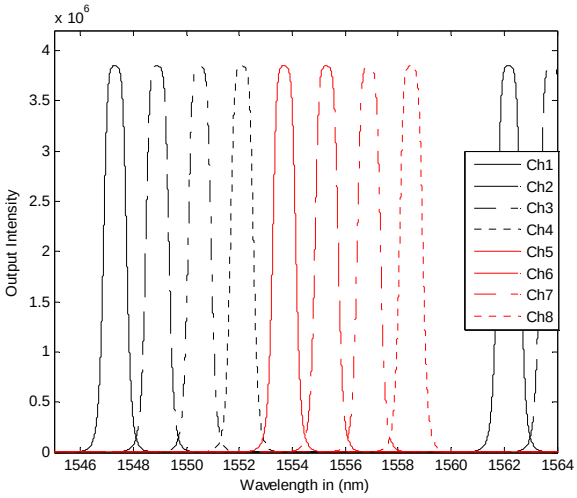

(b)

Fig. 2 Output characteristics of eight-channel serially coupled multi-stage racetrack ring resonator arrays with no load

Fig. 2 shows the output intensities as a function of wave length at the drop port and it has been achieved a line width of 0.8974nm in the reference ring resonator with a flat top pass band at 1dB of 0.5205nm and free spectral range of about 14.9nm. Also, it has been observed a line width incremental of 0.0009nm for the successive channel which results a change in the flat top pass band at 1dB of 0.0005nm in each successive channel.

C. Piezoelectric Actuated Beam

The geometry in Fig. 1 was analyzed using numerical simulations with Comsol Multiphysics finite element modelling software. Each beam comprised optimal design demission of a 30µm(l) x 300µm(w) x 2µm(h) a sandwiched silicon dioxide (SiO_2) cantilever beam, with a buried piezoelectric material of 1.6µm thickness(H) to get negligible displacement in the middle of the beam in both the y and z components as shown in Fig. 3 where, l, w *and* h represent the length, width and thickness of the beam, respectively.

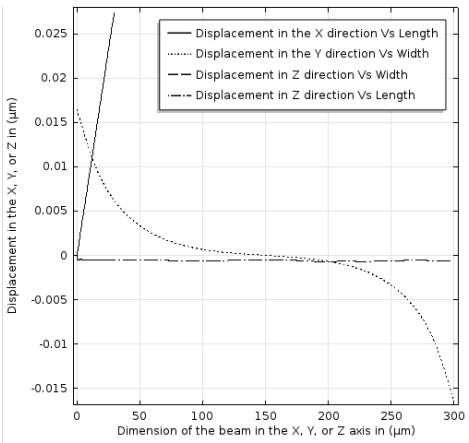

Fig. 3 Displacement in the X, Y and Z component of the beam

The DC voltage applied to the electrodes causes each beam to develop stress and strain. Thus, for thin silicon, ignoring the sheer stress and normal stress effect on optical performance, the longitudinal stress (T_i) and transversal stress (T_j) in the middle of each beam can be defined as:

$$T_i = E.d_{33}.\left(\frac{V}{l}\right).\left(\frac{H}{h}\right) T_j = E.d_{31}.\left(\frac{V}{l}\right).\left(\frac{H}{h}\right) \quad (9)$$

where, E is young's modulus, d_{33} and d_{31} is longitudinal and transverse piezoelectric coefficients of the material, respectively.

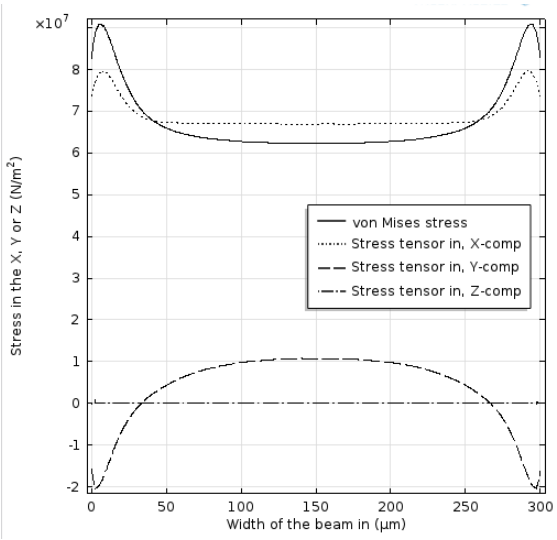

(a)

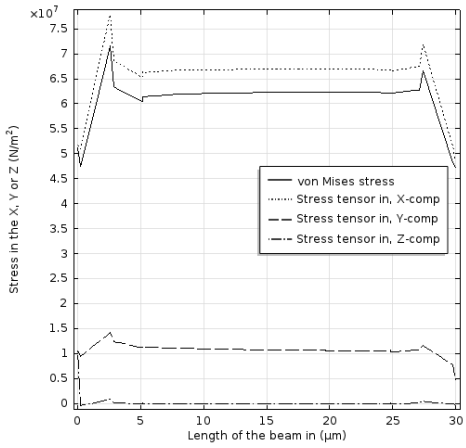

(b)

Fig. 4 Stress tensor in the X, Y or Z component versus (a) Width of the beam (b) Length of the beam

Figs. 4 (a) and (b) show the stress tensor in the X, Y or Z component of each beam for maximum applied voltage of +60V. In both case, it shows that, the stress is uniform across the middle of the beam and varies as it approaches to the

edges. Hence, the resonators' waveguides is located there to gain uniform refractive index change in each waveguide.

Similarly, strain can be defined as

$$\frac{\Delta l}{l} = \left(\frac{T_i(1-v^2)}{E}\right) \quad (10)$$

$$\frac{\Delta w}{w} = \left(\frac{T_j - vT_i}{E}\right) \quad (11)$$

This tells us that, as the applied voltage increases the longitudinal strain increase. Which intern affects the coupling length and the shape of the rings whereas, the transverse strain is almost zero in the middle, as it is shown in Fig. 5, which has insignificant effect on the inter waveguide gap and the shape of the rings where, v is Poisson's ratio.

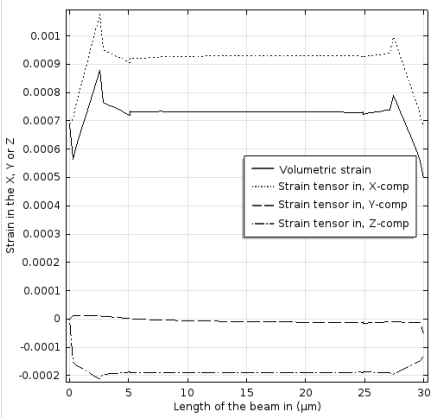

Fig. 5 Strain tensor in the X, Y or Z component versus length of the beam at +80V

D.Piezoelectric Actuated Beam

Due to stress-optic effect, the refractive index of the waveguide changes in each ring, it changes n_{eff} by Δn_{eff} in the rings. If we take the stress effect in each position of the ring into consideration, there is a uniformity in its refractive index change, thus, the effective refractive index change is related to the uniform stress in the surface of each beam through a fourth rank photo-elastic tensor as follows

$$\Delta n_{eff} = c.T_i(1-v) \quad (12)$$

where $C = 1.66 \times 10{-}11/Pa$ for the silicon core waveguide. RI change is directly proportional to the stress in each beam.

In addition to that, the longitudinal strain in each beam leads into two major effects:

i) elongation of the coupling length(L_c), which intern brings a change in the coupling efficiency.

$$L_c = (l + \Delta l).\frac{L_{c0}}{l} \quad (13)$$

ii) the change of the shape of the semi-circular parts of rings to an elliptical one. Thus, the cumulative phase change on the ring is given by

$$\Delta\emptyset = \frac{2\pi}{\lambda}(\Delta n_{eff}(2\pi R + 2L_{c0}) + n_{eff}\Delta P_V) \quad (14)$$

$$\Delta P_V = 2(L_c - L_{c0}) + \left(P_{ellipse} - 2\pi R\right) \quad (15)$$

where ΔP_V is change in the total circumference of the ring due to applied voltage and P_{elipse} is the circumference of the curves in both sides of the couplers.

III. Result

Thus, the resonance wavelength shift $\Delta\lambda_V$ as a function of effective refractive index change and the total circumference change of the ring ΔP_V can be written as

$$\Delta\lambda_V = \frac{2(\Delta n_{eff}(2\pi R + 2L_{c0}) + n_{eff}\Delta P_V)}{m} \quad (16)$$

where, m is the mode number and it is to be m=52.

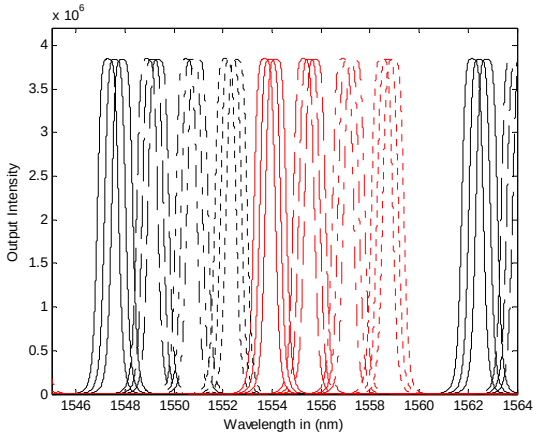

Fig. 6 Frequency response of output intensity of eight-channel tunable filter for an applied voltage with incremental of 5V

To investigate tunability of a multi-channel filter in our design, we actuated each beam. When controlling the actuation voltage of each beam simultaneously, input range from (0 to 60) V, Fig. 6 shows the transmission spectra versus input wavelength variation for an applied voltage of different values at the drop port of each channel. The curve shows the tunability of the optical filter with in the incremental of 5V of applied voltage. It is observed from the graph that there is a change in the typical parameters as it is shown in Table I. The bandwidth variation with an incremental of 0.0009nm from its' adjacent channel has been observed due to the change in perimeter and strain effect on the rings. It results a tenability variation of 0.05pm in each channel. A simultaneous linear variation of the wavelength shift as high as 45.54 pm/V has been achieved with a negligible tunablity variation in the eight channel tunable optical filter proportional to the DC voltage applied in the structure, and it is capable of tuning up to 3.45 nm in each channel with a maximum loss difference of 0.22dB in the tuning range.

TABLE I
TYPICAL CHANNEL PARAMETERS FOR THE EIGHT CHANNELS TUNABLE OPTICAL FILTER

Channel	1	2	3	4	5	6	7	8
Center wavelength (nm)	1547.3028	1548.9008	1550.4989	1552.0969	1553.6949	1555.2930	1556.8910	1557.1194
1dB bandwidth (nm)	0.5205	0.5210	0.5215	0.5220	0.5225	0.5230	0.5235	0.5240
3dB bandwidth (nm)	0.8974	0.8983	0.8992	0.9001	0.9010	0.9019	0.9028	0.9037
Tunability (pm/V)	45.42	45.46	45.5	45.54	45.58	45.62	45.66	45.70
Spacing (nm)	1.598							
Loss difference (dB)	0.2218							
Band rejection ratio (dB)	35							
Channel crosstalk (dB)	< 30							
Tuning Range (nm)	3.45							

IV. CONCLUSION

We have proposed and analysed novel eight-channel piezoelectric (PZT) actuated tunable optical filter based on racetrack multi-ring resonators for the first time for wavelength de-multiplexing applications. We design tunable eight-channel wavelength de-multiplexer consists of eight cascaded PZT actuated tunable multi-ring resonator filters with a channel spacing of 1.6nm. A small change in the perimeters of the rings is introduced to establish the shift in resonance wavelength according to the defined channel spacing and it has been achieved a negligible tunablity variation with a flat top pass band incremental at 1dB of 0.0005nm. Also, the effects of the coupling coefficients on each resonance are investigated. Moreover, the piezoelectric actuated beam is optimally designed to maximize the uniform stress on the middle of the beam and linearly varying strain along the length while reducing strain in the other direction.

The wave length shift as high as 45.54pm/V has been achieved in eight channel tunable optical filter proportional to the DC voltage applied in the structure, and it is capable of tuning up to 3.45nm in each channel with a maximum loss difference of 0.22dB in the tuning range and out of band rejection ratio of 35dB, with a low channel crosstalk ≤ 30 dB.

ACKNOWLEDGMENT

First author (Hailu Dessalegn) wishes to thank Department of Electrical Communication Engineering, Indian Institute of Science for giving an opportunity and providing the necessary facility. Second author (T. Srinivas) wishes to acknowledge Indian Institute of Science for providing financial assistance to attend the conference.

REFERENCES

[1] D. C. Kilper, R. Bach, D. J. Blumenthal, D. Einstein, T. Landolsi, et al., "Optical Performance Monitoring" Journal of Light wave Technology, Vol. 22, NO. 1, pp. 294–304, January 2004.
[2] Wim Bogaerts*, Peter De Heyn, Thomas Van Vaerenbergh, Katrien De Vos, Shankar Kumar Selvaraja, et al., "Silicon microring resonators," Laser Photonics Rev. 6, No. 1, pp. 47–73, 2012.
[3] B D Timotijevic, F Y Gardes, W R Headley, G T Reed, M J Paniccia, et al., "Multi-stage Racetrack Resonator Filters in Silicon-on-Insulator", Journal of Optics A: Pure and Applied Optics 8(2006) S473-S476.
[4] Shijun Xiao, Maroof H. Khan, Hao Shen and Minghao Qi, "Multiple-Channel Silicon Micro-resonator based Filter for WDM Applications", Vol. 15, No. 12 Optical Society of America, 2007
[5] Fenfei Liu and Mani Hossein-Zadeh, "On the Performance of High-Q Multiring Optical Filters", IEEE Photonics Journal, 2010.
[6] Jin Yao, Ming-Chang M. Lee, David Leuenberger and Ming C. Wu, "Wavelength- and Bandwidth-Tunable Filters Based on MEMS-actuated Microdisk Resonators", Optical Society of America, 2005.
[7] Tarek Mamdouh and Diaa Khalil, "A MEMS Tunable Optical Ring Resonator Filter", Optical and Quantum Electronics, 37:835–853, 2005.
[8] Dooyoung Hah, John Bordelon, and Dan Zhang, "Mechanically Tunable Optical Filters with a Microring Resonator", Optical Society of America, 2011.
[9] Jun Rong Ong, Ranjeet Kumar, and Shayan Mookherjea, "Ultra-High-Contrast and Tunable-Bandwidth Filter Using Cascaded High-Order Silicon Microring Filters", IEEE Photonics Technology Letters, Vol. 25, No. 16, 2013.